PLOS | ONE

RESEARCH ARTICLE

Graded Maximal Exercise Testing to Assess Mouse Cardio-Metabolic Phenotypes

Jennifer M. Petrosino[1,7], Valerie J. Heiss[1], Santosh K. Maurya[2], Anuradha Kalyanasundaram[3], Muthu Periasamy[2], Richard A. LaFountain[1], Jacob M. Wilson[4], Orlando P. Simonetti[5,6], Ouliana Ziouzenkova[1]*

1 Department of Human Sciences, The Ohio State University, College of Education & Human Ecology, Columbus, Ohio, United States of America, **2** Cardiovascular Pathobiology Program, Sanford Burnham Medical Research Institute at Lake Nona, Orland, Florida, United States of America, **3** Department of Physiology and Cell Biology, The Ohio State University College of Medicine, Columbus, Ohio, United States of America, **4** Department of Human Performance, The University of Tampa, Tampa, Florida, United States of America, **5** Department of Radiology, The Ohio State University, College of Medicine, Columbus, Ohio, United States of America, **6** Department of Cardiovascular Medicine, The Ohio State University, College of Medicine, Columbus, Ohio, United States of America, **7** Biomedical Sciences Program, The Ohio State University, College of Medicine, Columbus, Ohio, United States of America

* ziouzenkova.1@osu.edu

OPEN ACCESS

Citation: Petrosino JM, Heiss VJ, Maurya SK, Kalyanasundaram A, Periasamy M, LaFountain RA, et al. (2016) Graded Maximal Exercise Testing to Assess Mouse Cardio-Metabolic Phenotypes. PLoS ONE 11(2): e0148010. doi:10.1371/journal.pone.0148010

Editor: Yann Herault, IGBMC/ICS, FRANCE

Received: August 14, 2015

Accepted: January 12, 2016

Published: February 9, 2016

Data Availability Statement: All relevant data are within the paper and its Supporting Information files.

Funding: This research was supported by Award Number 20020728 from American Egg Board and Award Number 10040042 from Novo Nordisk Pharmaceuticals, as well as by the Food Innovation Center (OZ, JMP). The project described was supported by Award Number R21OD017244 (OZ), UL1TR001070 (CCTS), UL1RR025755 and NCI P30CA16058 (OSUCCC) from the National Center for Research Resources, funded by the Office of the Director (OD), National Institutes of Health and supported by the NIH Roadmap for Medical

Abstract

Functional assessments of cardiovascular fitness (CVF) are needed to establish animal models of dysfunction, test the effects of novel therapeutics, and establish the cardio-metabolic phenotype of mice. In humans, the graded maximal exercise test (GXT) is a standardized diagnostic for assessing CVF and mortality risk. These tests, which consist of concurrent staged increases in running speed and inclination, provide diagnostic cardio-metabolic parameters, such as, VO_{2max}, anaerobic threshold, and metabolic crossover. Unlike the human-GXT, published mouse treadmill tests have set, not staged, increases in inclination as speed progress until exhaustion (PXT). Additionally, they often lack multiple cardio-metabolic parameters. Here, we developed a mouse-GXT with the intent of improving mouse-exercise testing sensitivity and developing translatable parameters to assess CVF in healthy and dysfunctional mice. The mouse-GXT, like the human-GXT, incorporated staged increases in inclination, speed, and intensity; and, was designed by considering imitations of the PXT and differences between human and mouse physiology. The mouse-GXT and PXTs were both tested in healthy mice (C57BL/6J, FVBN/J) to determine their ability to identify cardio-metabolic parameters (anaerobic threshold, VO_{2max}, metabolic crossover) observed in human-GXTs. Next, theses assays were tested on established diet-induced (obese-C57BL/6J) and genetic (cardiac isoform *Casq2*$^{-/-}$) models of cardiovascular dysfunction. Results showed that both tests reported VO_{2max} and provided reproducible data about performance. Only the mouse-GXT reproducibly identified anaerobic threshold, metabolic crossover, and detected impaired CVF in dysfunctional models. Our findings demonstrated that the mouse-GXT is a sensitive, non-invasive, and cost-effective method for assessing CVF in mice. This new test can be used as a functional assessment to determine the cardio-metabolic phenotype of various animal models or the effects of novel therapeutics.

Research. The content is solely the responsibility of the authors and does not necessarily represent the official views of the National Center for Research Resources or the National Institutes of Health.

Competing Interests: The authors state that their commercial funding does not alter their adherence to PLOS ONE Editorial policies and criteria.

Abbreviations: APMHR, age-predicted maximal heart rate; AT, Anaerobic threshold; $Casq2^{-/-}$, Cardiac calsequestrin deficient mice; CAD, Coronary artery disease; GXT_h, Human graded maximal exercise test; GXT_m, Mouse graded maximal exercise test; LA, Lactate; PDH, Pyruvate dehydrogenase; PXT_m, Mouse progressive maximal exercise test; RER, Respiratory exchange ratio; RPE, rating of perceived exertion; RR, respiratory rate; VO_2, Volume of oxygen consumed; VO_{2max}, Maximal oxygen consumption; WT, Wild type.

Introduction

Obesity rates are rising exponentially and increase patients' risks for developing cardiovascular diseases [1]. Heart disease remains the leading cause of death in the United States and worldwide. Subsequently, this has stimulated a large interest in understanding the metabolic and physiological mechanisms regulating cardiovascular function and energy balance. For over 50 years, human research has used graded maximal exercise testing (GXT_h) as the prototypical method to study cardiovascular and metabolic responses of the body to stress [2–4]. These standardized GXT_h tests, such as the gold standard Bruce protocol [5, 6], are key non-invasive and cost-effective methods for the assessing patient mortality risks [7, 8] and diagnosing coronary artery disease (CAD) [9].

New therapies for metabolic and cardiovascular disease have fast progressed with the development of genetic mouse models of cardiovascular dysfunction (reviewed in [10–14]). Genetic models, like the low-density lipoprotein receptor ($Ldlr^{-/-}$) [11], apolipoprotein E ($ApoE^{-/-}$) [15], and endothelial nitric oxide synthase ($eNos3^{-/-}$) [16] knockout mice are well studied models of atherosclerosis. Similar to obese humans, diet-induced obese wild-type mice (WT-obese; C57BL/6J) can develop fatty streaks [17], left ventricular hypertrophy, and cardiac fibrosis [18–20]. Additionally, the WT-obese mouse model phenocopies the insulin resistant state, and subsequent impaired delivery of nutrients to skeletal muscles [21], that is seen in obese individuals during exercise testing [22]. Some knockout models are generated from mutations observed in patients with impaired cardiovascular function. These mouse models often phenocopy human mutations, develop cardiac dysfunction, and can be used to generate highly translatable findings. For example, the calsequestrin 2 (cardiac specific isoform) deficit mouse ($Casq2^{-/-}$) phenocopies humans with CASQ2 mutations. Both $Casq2^{-/-}$ mice and patients with CASQ2 mutations develop arrhythmias [23], catecholaminergic ventricular tachycardia, and can be diagnosed with exercise testing [24, 25]. Given the ability of mouse models to phenocopy various aspects of cardiovascular disease, the use of mouse models has become critical to the study of cardiac biology, physiology, and novel therapeutics prior to translating findings to man [10, 12–14, 26].

As a result of the expanding number of mouse models used to study metabolic and cardiovascular disease, animal exercise testing has become widely published [27–54] as a way to functionally characterize the cardiovascular fitness (CVF) of mice [55–58]. Maximal exercise testing is designed to induce specific stress to working muscles and the heart. During testing, cardiac output primarily drives the associated increase in oxygen consumption (VO_2) until maximal oxygen consumption (VO_{2max}) and exhaustion is achieved. This resulting state of VO_{2max} is characterized by sympathetic dominance, parasympathetic inhibition [59], and vasoconstriction to all systems but the heart, brain, and working muscles. While there are many conserved physiological responses between the cardiorespiratory systems of mice and men exposed to stress [60], there are also many differences that must be understood to enhance the interpretation and design of mouse exercise testing. The mouse heart is small (~0.2 g), beats between 400–600 beats per minute (bpm), and has a cardiac output (heart rate x strove volume) that is 2x-9x greater than humans. Differentially, the human heart is large (~250–300 g) and beats between 60–90 bpm at rest. Interestingly, when mouse and human stroke volume is normalized to bodyweight, there is not much discrepancy between the values recorded (reviewed in [13, 60, 61]). Many of the differences between human and mouse cardiac physiology are due to differences in heart size and rate, body mass, and oxygen requirements (reviewed in [60]). As a result, the information from exercise testing in mice and men will never be identical. Nonetheless, a lot of information can be generated from mouse treadmill

tests with calorimetry data reporting, so long as the following established GXT_h considerations are adapted to mouse testing protocols:

1. modest stage to stage increases in energy requirements
2. a testing duration greater than 6 minutes
3. a test lasting no longer than 12 minutes [2, 62] and
4. appropriate acclimation of animals to treadmills.

Without these considerations, tests may lack the appropriate intensity needed to accurately assess the CVF of mice.

Currently, exercise testing in mice and men diverge in the areas of test design, time of test, and parameters that can be reported. GXT_h tests have staged concurrent increases in speed and inclination over the course of 8–12 minutes [9]. However, unlike with human testing, there are no standardized protocols or end point criteria for positive tests in mice. Most rodent assays are designed with increasing speed over a fixed inclination (defined as PXT_m) for time periods greater than 12 minutes [23, 58, 63–69]. The most common variables reported in animal assays include VO_{2max}, run time, and maximum run speed; which may not be sufficient for detection of impaired CVF [23]. Human testing differs in that it can derive additional diagnostic cardio-metabolic parameters such as anaerobic threshold (AT) [70], crossover (the shift from lipid to carbohydrate oxidation [71]), and pre- to post-test changes in lactate concentrations ($Lactate_{delta}$) [72]. These variables provide valuable information regarding the ability of the cardiac and pulmonary systems to deliver oxygen (O_2) during maximal and submaximal exercise intensities [73]. However, these parameters are rarely, if ever, reported in mouse testing because they cannot be accurately derived. Failure to derive these variables questions the ability of these assays to accurately assess mouse CVF. This, along with other limitations in currently utilized protocols (reviewed in [55, 74]), point out the need for a more efficacious and reliable standardized approach to test mouse CVF.

Here, we developed a new exercise testing method, the graded mouse maximal exercise test (GXT_m) and describe how to derive novel diagnostic cardio-metabolic parameters in mice that can be generated from data acquired during maximal exercise testing. Additionally, we compare a new GXT_m to a PXT_m, and the human GXT_h. Our results showed that in mice, only the GXT_m was capable of generating cardio-metabolic parameters previously reported in human testing and consistently detecting impaired CVF in established mouse models of cardiovascular dysfunction.

Methods

Human Studies

Study Approval. For human testing, all subjects gave written informed consent prior to participation and all tests were done in accordance with procedures approved by The Ohio State University Biomedical Institution Review Board for this study. All animal experiments in this study were performed in accordance with procedures approved by Ohio State University Institutional Animal Care and Use Committee (IACUC) committee for this study and in accordance with the National Institutes of Health guidelines.

Human Bruce protocol testing (GXT_h). Healthy, recreationally trained men between 18 to 45 years of age were recruited from Columbus, Ohio to complete a Bruce protocol graded maximal treadmill exercise test following acclimation to test ($n = 6$). Testing was performed using ParvoMedics TrueOne 2400 systems and ParvoMedics software. ParvoMedics 2400 metabolic cart was turned on and allowed to warm up for at least thirty minutes prior to calibration

and testing procedures. Pneumotachometer and gas analysis systems were calibrated according to manufacturer instructions before use during exercise testing. Expired gas was continuously sampled during exercise, through a 61cm Nafion tube (Permapure, Toms River, NJ, USA), via paramagnetic oxygen analyzer (0–25% range with 0.1% accuracy) and an infrared carbon dioxide analyzer (0–10% range with 0.1% accuracy). Metabolic data was sampled using 15 seconds averaging. Testing stages consisted of simultaneous increases in speed and inclination as previously described [6] (Table 1). All human subjects were required to achieve at least three of the following criteria indicating $\dot{V}O_2$max was reached: plateauing of oxygen consumption ($\dot{V}O_2$), respiratory exchange ratio (RER) $\geq$ 1.1, heart rate $\geq$ 95% age-predicted maximal heart rate (APMHR), rating of perceived exertion (RPE) $\geq$ 17, respiratory rate (RR) $>$ 40 breaths per minute, or subject inability to continue.

Animal Studies

Animal subjects studied. Mice were housed with 12-hour light and dark cycles and maintained on a standard chow diet. C57BL/6J (WT, *n* = 7), FVB/NJ (Jackson Laboratories, Bar

Table 1. VO_{2max} testing protocols in mice and men.

PXT_m	Speed	Incline	Duration
Stage	(meter/min)	(% grade)	(min)
1	6	0	5
2	7	0	0.5
3	8	0	0.5
4	9	0	0.5
5	10	0	0.5
6	11	0	1
7	12	0	2
8	13	0	2
9	14	0	2
10	15	0	2
11	16	0	1
GXT_h	Speed	Incline	Duration
Stage	(km/hr)	(% grade)	(min)
1	2.7	10	3
2	4	12	3
3	5.4	14	3
4	6.7	16	3
5	8	18	3
6	8.8	20	3
7	9.6	22	3
GXT_m	Speed	Incline	Duration
Stage	(meter/min)	(% grade)	(min)
1	9	5	2
2	12	10	2
3	15	15	2
4	18	15	1
5	21	15	1
6	23	15	1
7	24.0+	15	1

Stages, speed, and incline of maximal exercise tests completed are described.

doi:10.1371/journal.pone.0148010.t001

Harbor, Maine, $n = 4$), obese C57BL/6J on high fat diet (45kcal/fat, Research Diets Inc, New Brunswick, NJ, ~100 days of high fat diet feeding, $n = 11$) and Calsequestrin 2 (cardiac isoform) null (*Casq2*$^{-/-}$, $n = 4$)(*Mus musculus*) [23, 75] male mice, 4–6 months old, were used. Metabolic and physiological parameters are described in S1 Table.

Animal acclimatization to treadmills. Animals were first acclimated (S2 Table) to the treadmill (Metabolic Modular Treadmill; Columbus Instruments, Columbus, OH, USA) and then rested for one week prior to performing the GXT_m. Acclimation consisted of 3 training sessions with 60 hours recovery between sessions. During acclimation mice were placed in a motionless treadmill for 3 minutes, after which the shock grid was activated (3 Hz and 1.5 mA). Next, the treadmill was engaged to a walking speed of 6 m/min for 5 minutes and progressively increased up to 12 m/min for a total duration of 12 minutes of exercise.

Software calibration and calculations from Metabolic Modulator Treadmill. Before each testing session, Oxymax software (Columbus Instruments, Columbus, OH, USA) and open circuit indirect calorimetry treadmills (Metabolic Modular Treadmill, Columbus Instruments, Columbus, OH) [76] were calibrated and checked for hardware malfunctions according to manufacturer instructions. Prior to calibration, sample pump was turned on with flow indicator showing flow set at 4–5 LPM. Pressure reading was set at ~800mmHg and gas tank output pressure was set at 10psi. Gas calibration was performed and adjusted when necessary using the GAIN and FINE knobs to set reading at 0.50% CO_2 and 20.5% O_2. Drierite (Calcium Sulfate with Indicator, Sigma-Aldrich; St. Louis, MO, USA) was changed constantly to maintain accurate gas readings and to assure that moisture accumulating during testing could properly be absorbed. During testing, analysis was set to collect gas exchange measures every 15 seconds (settings: cage settle was set to every 15 sec; cage measure was set to every 15 sec; reference settle was set to every 30 sec; reference measure was set to every 30sec, volume rate unit was set to ml/kg/min, and accumulated gas unit was set as liter). During experiments, system sample pump maintained a constant sample flow reading of 0.5 L/min and sample drier a purge gas flow reading of 1.5 L/min. Maximum run speed (meter/min), shock grid contact (seconds) and time until exhaustion (min) were manually recorded with stopwatch. Oxymax computer software collected gas concentrations and flow to calculate oxygen consumption (VO_2), carbon dioxide expiration (VCO_2), and RER (VCO_2/VO_2) from the treadmill every 15 sec. Oxymax gas exchange calculations and generation of RER derived fuel substrate oxidation are additionally listed in the supplementary materials (S2 Text, S3 Table).

Mouse Graded Maximal Exercise Test (GXT_m). Following one week of rest from acclimation training, mice were placed on the treadmill at 0° incline and the shock grid was activated. The treadmill speeds were then increased until exhaustion as follows: (speed, duration, grade)—(0 m/min, 3 min, 0°), (6 m/min, 2 min, 0°), (9 m/min, 2 minutes, 5°), (12m/min, 2 min, 10°), (15m/min, 2 min, 15°), (18, 21, 23, 24 m/min, 1 min, 15°), and (+1 m/min, each 1 min thereafter, 15°). Exhaustion (endpoint for treadmill cessation) was defined as the point at which mice maintained continuous contact with the shock grid for 5 seconds. Continuous contact is defined as any portion of the animal's body coming in contact with the shock grid for a total of 5 seconds. During the test, occasional (~1–5 times per single animal test) 1–2 second tail contacts were observed when animals misstepped or were slow to response in the increase in intensity. VO_{2max} was determined by the peak oxygen consumption reached during this test when RER was >1.0. Maximum running speed was defined as the treadmill speed at which VO_{2max} was achieved (Table 1). All animals (within-subjects design, GXT_m and PXT_m) underwent pre- and post-test lactate assays (Lactate assay) one hour prior to and immediately following exercise testing).

Mouse Progressive Maximal Exercise Test (PXT_m). Following one week of rest after GXT_m the PXT_m was conducted as described in [56]. Specifically, mice were placed on the

treadmill (0° incline entire experiment) and the shock grid was activated. The treadmill speeds were then increased until exhaustion as follows: (speed, duration)—(0 m/min, 5 min), (6 m/min, 5 min), (7, 8, 9, and 10 m/min, 30s each), (11m/min,1 min), (12, 13, 14, and 15 m/min, 2 min each), and (+1 m/min, each 1 min thereafter). Exhaustion (endpoint for treadmill cessation) was defined as the point at which mice maintained continuous contact with the shock grid for 5 seconds (further described in the GXT_m section). $VO_{2\ max}$ was determined by the peak oxygen consumption reached during this test when RER was $\geq$ 1.0. Maximum running speed was defined as the treadmill speed at which VO_{2max} was achieved. All animals (within-subjects design, GXT_m and PXT_m) underwent pre- and post-test lactate assays one hour prior to and immediately following exercise testing).

Lactate assay. A protocol [77] was adapted to measure venous blood lactate concentrations from the tail vein. During acclimation exercise sessions, mice were also acclimated to tail vein blood collection (3 pre acclimation session collections, and 3 post acclimation session collections). For the PXT_m and GXT_m; 1 hour prior to testing, ~0.7μL of blood (via tail vein prick) was collected and placed for analysis on a handheld lactate meter (Lactate Plus; Nova Biomedical, Waltham, MA, USA). Within one minute of test completion, ~0.7μL of blood was again collected and analyzed. For all testing, the same device was utilized to reduce variability.

Statistical Analysis. Data processing: Prior to analysis, the dependent variables with the four genotypes (WT, WT obese, *Casq2*$^{-/-}$, FVB/NJ) and two test types (GXT_m, PXT_m) were examined through IBM SPSS version 22 (9.5.0.0) for accuracy of data entry, fit between their distributions, and the assumptions of multivariate analysis. Upon inspection of standardized scores, there were no univariate outliers. Mahalanobis distance values were requested and no multivariate outliers were identified as exceeding the Mahalanobis distance value at $p < .01$ ($\chi^2 = 32.00$, $df = 16$, $p = .01$). Therefore, no additional cases were removed from the dataset. A review of plots of the residuals for each of the five dependent variables by group indicated that the assumption of independence was satisfied. Pairwise linearity was checked to determine the relationship between dependent variables using within-group scatterplots and also found to be satisfactory. All skewness and kurtosis statistics were between the range of -2 and 2, providing evidence that normality was a reasonable assumption. Further evidence of normality can be seen through the visible inspection of Q-Q plots and histograms of each dependent variable. There were no issues with normality observed.

Analyses and statistical tests: were performed with IBM SPSS Statistics 22 (9.5.0.0). All values represent mean SD unless noted otherwise. Two-Three group MANOVAS were performed. The Bonferroni correction when applied to an alpha of .05 yielded an alpha level of .007 for the univariate ANOVAs and Tukey HSD Multiple Comparisons presented. When appropriate, Student's two-tailed *t*-test were applied with *P*-values <0.05 being considered significant. The results of the ANCOVA tests, with weight as a covariant, for the calorimetry data (VO_2 data) and information regarding statistical test selection for calorimetry data analysis is further described in S3 Text.

Results

Development of a GXT_m exercise assay for mice

Our goal was to develop a test for mice that provided cardio-metabolic parameters previously reported in the human GXT_h and to compare those parameters describing mouse performance during both the GXT_m and PXT_m. We used lean WT (C57BL/6J) male mice as a control group, C57BL/6J male mice with diet induced obesity (WT-Obese) as a non-transgenic model of cardiac deficiency [18–20, 78], and calsequestrin 2 (cardiac isoform) deficient (*Casq2*$^{-/-}$) male mice as a genetic model with reported cardiac deficiency [23, 75] (S1 Table). During the study,

no animals experienced adverse effects from exercise testing that required them to be removed early from testing.

Within-subjects design for PXT_m and GXT_m was used to reduce errors associated with individual differences. Examples of representative single tests and the averaged measurements of all tests are shown in S1 and S2 Figs. Initially, we performed the GXT_m and the PXT_m using control WT male mice and the GXT_h using healthy male human subjects. For all protocols, both mouse and human subjects underwent acclimation prior to testing. In mice, following the GXT_m, an additional week of rest was given before animals performed the PXT_m. This was done to minimize the effect of training induced adaptations. Of note, we performed the testing in opposite order and found no differences in performance (data not shown). Additionally, all mice underwent pre- and post-test lactate (LA) assays one hour prior to and following test termination (~within one minute of treadmill stopping and animal being removed) as biochemical confirmation that exhaustion was achieved.

We developed the GXT_m protocol taking into consideration that most PXT_m tests [23, 58, 63–69, 79–83] increase the speed at a set incline over time (Table 1, Fig 1A) until maximal exertion and a respiratory exchange ratio (RER, the quotient of (VCO_2/ VO_2) $\geq$ 1.0 is achieved (S4 Table). VO_{2max} testing is limited by the ability of the cardiorespiratory system to supply oxygen to working muscles. Experiments altering oxygen delivery (hypoxia), overperfusing muscles during exercise, and showing the contributions of cardiac output relative to arterial-venous oxygen (reviewed in [84]) have been key in determining this concept. Accordingly, both the human and mouse GXT were designed to promote an end stage in which VO_2 fails to rise as oxygen demands increase. This end state is marked by predominately cardiac fatigue and an enhanced dependence on anaerobic glycolysis [84] prior to the onset of skeletal muscle exhaustion.

In our human GXT_h and established GXT_h protocols (Table 1), there are simultaneous staged increases in speed and incline until the following conditions are met [9]: 1) maximal exertion, 2) achievement of RER $\geq$ 1.1, 3) a plateau or decrease following peak oxygen consumption, 4) a significant increase in pre- to post-test venous blood LA concentrations (~8-10mmol/l), and 5) failure of heart rate to increase with increasing exercise intensity (S4 Table). We developed a similar, but not identical, GXT test in mice (GXT_m) by have stages of simultaneous increases in speed and incline to achieve: 1) maximal exertion, 2) achievement of RER $\geq$ 1.0, 3) a plateau or decrease following peak oxygen consumption, and 4) a significant increase in post-test venous LA concentrations (~8mmol/l). Treadmill inclination increases, which were restricted to 5° increments, were capped at 15° due to observations in initial method development which showed that mice struggled to maintain natural gait with incline set >15°. The end points of all exercise tests are described in S5 Table. In mice, maximal exertion on the test was measured as time until exhaustion (minutes), and determined by $\geq$ 5 seconds of continuous contact with the shock grid. Continuous contact was defined as any portion of the animal's body coming into contact with the shock grid. It should be noted that rarely were animals seen sitting down on the shock grid. Instead, most continuous contacts consisted of the animal's tail or hind limb partially contacting the shock grid. Exhaustion was further validated using biochemical measures of circulating LA concentrations.

Reported measures in healthy mice and man during exercise testing

Oxygen consumption (VO_2) and carbon dioxide expiration (VCO_2) were two principal measures obtained from the metabolic treadmill (S1 and S2 Texts) during testing. In healthy WT mice, both the PXT_m and GXT_m showed increases in VO_2 and VCO_2 during testing (Fig 1B); however, in the majority of single PXT_m tests, VCO_2 and VO_2 did not intersect at VO_{2max}. This

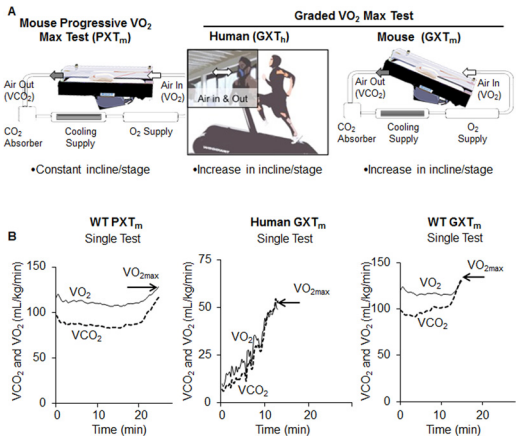

Fig 1. Description of exercise testing in mice and men. (A) Schematic description of exercise testing in mice and men. The PXT_m maintains fixed inclination (0°) while speed increases until the test is terminated (Table 1). Training in mice was done on a chamber-enclosed treadmill that allowed it to function as an open circuit indirect calorimeter; and thus, allowed for derivation of VO_2 and VCO_2 values. With the GXT_m (middle) and GXT_h (right), speed and incline simultaneously increased as stages progressed (Table 1). (B) Human and mouse tests used indirect calorimetry to measure VO_2 (solid line) and record VO_{2max} as well as measure CO_2 (dashed line). Mouse and man tests were randomly selected from WT males (*n* = 7) and healthy men (*n* = 6) and used for derivation of all parameters (all data are shown in S1 and S2 Figs). During maximal exercise testing both species have similar responses (RER, lactic acid formation, fuel utilization, O_2 use, heart rate, speed, exhaustion). In the GXT_m, and GXT_h. at VO_{2max}, VCO_2 intersected or surpassed VO_2, and was a parameter of a positive test (as RER >1.0, middle and right panel). In the PXT_m, VO_{2max} did not fulfill this criterion (left panel).

doi:10.1371/journal.pone.0148010.g001

suggested that true maximum was not achieved. In the GXT_m, all single tests showed a clear intersection of VCO_2 and VO_2.

Time until exhaustion lasted for 20 to 29 minutes with PXT_m excluding warm-up (Fig 1B). The most commonly used GXT_h, the Bruce protocol, elicits time until exhaustion between 8–12 minutes in the general population [4, 5, 9]. Similarly to the reported data, our GXT_h and GXT_m tests achieved exhaustion between 8–12.5 minutes in WT mice and healthy humans (excluding warm-up) (Fig 1B). Furthermore, the GXT_m data consistently produced VO_{2max} values that were accompanied by exhaustive efforts and increased blood LA concentrations. Significant elevation of blood lactate post-test is a marker for the transition from aerobic to anaerobic metabolism and only consistently occurred in GXT_m (data for all mouse groups are shown and discussed later).

RER was used to determine anaerobic threshold (AT) and fuel substrate (carbohydrate and lipid) oxidation (S3 Table) during testing. Anaerobic threshold (AT) is the point at which there is a shift from aerobic to anaerobic metabolism and signifies the onset of metabolic acidosis during continuous exercise [85]. The standard method for determining AT in humans is through multiple blood draws while running. This determination method was not feasible to execute in mice constrained in an enclosed metabolic treadmill. Thus, we determined AT using the method of identifying an abrupt increase in RER kinetics [85] and were able to consistently determine AT from RER kinetics in both human and mouse GXT single tests (Fig 2A).

AT was more difficult to consistently determine from single PXT_m tests, and in those where it could be determined, it occurred approximately 20 minutes or longer into the test compared to the GXT_m. Using RER values, we were also able to calculate a previously established GXT_h parameter known as the crossover point (the transition from fat to carbohydrate oxidation [71]). Each single GXT_m test and averaged test allowed for crossover determination (Fig 2B); however, a specific crossover point could not be determined from most single PXT_ms (Fig 2B).

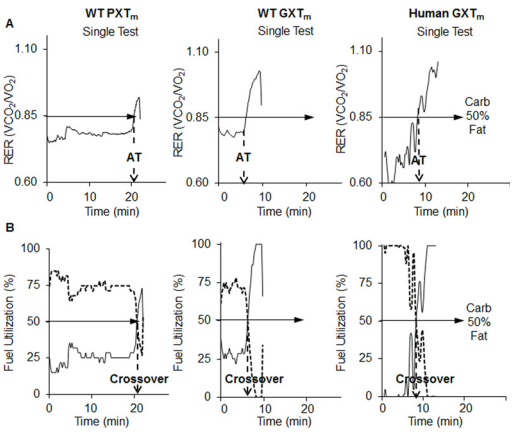

Fig 2. Kinetics and parameters from PXT_m, GXT_m, and GXT_h using single test analysis. The same single mouse and man tests were randomly selected from WT males (n = 7) and healthy men (n = 6) and used for derivation of all parameters. (A) RER (VCO_2/ VO_2) represents fuel substrate utilization during PXT_m, GXT_m, and GXT_h. An RER of .85 (solid horizontal arrow) indicates 50% carbohydrate and 50% fat oxidation. In a single test, the point in which there is an abrupt increase in RER is known as anaerobic threshold (AT, dashed arrow). (B) Carbohydrate (dashed line) and fat (solid line) oxidation was determined from RER values (S6 Table) in the PXT_m, GXT_m, and GXT_h. Dotted vertical arrow indicates the crossover time point in the test where there is a shift from predominant lipid oxidation to predominate carbohydrate oxidation.

doi:10.1371/journal.pone.0148010.g002

Crossover could be determined from the averaged PXT_m (Fig 2B). In the averaged GXT_m, compared to the averaged PXT_m, crossover occurred sooner and at a similar time point to the GXT_h (S1 Fig). Of note, cardio-metabolic parameters (VO_2, VCO_2, RER, AT, crossover) were derived from single tests, and then averaged, when completing analysis. Our findings indicated that longer tests with progressive intensity increases, like the PXT_m, were not capable of producing VO_{2max} with associated biochemical increases in lactate and parameters specific to an increased reliance on the glycolytic system (crossover, AT). These measures were; however, reported in both healthy mice and men during the GXTs.

Sensitivity of mouse testing methods to detect impaired cardiovascular fitness

Next, we quantitatively compared PXT_m and GXT_m tests in dysfunctional mouse models to assess their sensitivity in detecting impaired levels of CVF. Averaged kinetics for VO_2 revealed differences among WT-lean, WT-obese, and *Casq2*$^{-/-}$ mice with the GXT_m. With the PXT_m, VO_2 kinetics was similar between the *Casq2*$^{-/-}$ and obese mice; with both strains failing to show a progressive increase in VO_2 over the course of the test (Fig 3A). Only the WT mice showed increases in VO_2 as the PXT_m progressed. With the PXT_m, relative VO_{2max} (VO_{2max} normalized to body weight) was only significantly suppressed in the obese group. Additionally, VO_{2max} was unchanged between the WT and the *Casq2*$^{-/-}$ (Fig 3B). With the GXT_m, relative VO_{2max} was significantly suppressed in both dysfunctional models (alpha = .007, MANOVA, Tukey HSD Multiple Comparisons; $p < .001$, WT v. obese; $p = .001$; WT v. *Casq2*$^{-/-}$; $p = .001$ obese v. *Casq2*$^{-/-}$; Fig 3B). Of note, an expected increase from basal VO_2 to VO_{2max} (VO_{2delta}) was achieved in all tests (PXT_m, GXT_m) with the exception of WT v. obese using the PXT_m (alpha = .007, MANOVA, Tukey HSD Multiple Comparisons; $p = .006$, WT v. obese; Fig 3C). However, this could have been observed as a result of the PXT_m eliciting a smaller VO_{2delta} in WT compared to the GXT_m ($p < .05$, Student's t-Test). We validated all data with an additional control strain (S5 and S7 Tables) to further confirm the sensitivity of each test.

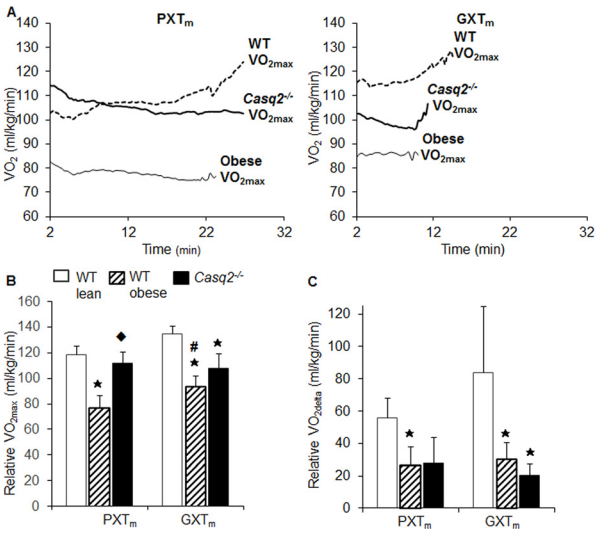

Fig 3. VO_{2max} achieved with the GXT_m, but not the PXT_m, identifies impaired cardiovascular fitness in mouse models of cardiovascular dysfunction. (A) Averaged VO_2 kinetics obtained from WT (dashed line), *Casq2*$^{-/-}$ (solid thick line), and obese (solid line) mice that performed the PXT_m and GXT_m. VO_2 is indicated for each group from the beginning of the test until the end (Minute 2, after the 2 minute warm, to point of exhaustion). Of note, during the PXT_m, the largest increase in VO_2 occurred with the first stage, and leveled off as the test continued in dysfunctional models. (B) Relative VO_{2max} values and (C) change from baseline to maximal oxygen consumption (VO_{2delta}) are compared (mean±SD, MANOVA, Tukey HSD Multiple Comparisons, alpha = .007) in WT-healthy (white bar), WT-obese (hashed bar), and *Casq2*$^{-/-}$ (black bar) mice. Asterisks indicate significance at the alpha = .007 level (MANOVA, multiple comparisons Tukey HSD for the PXT_m and GXT_m of WT v. obese and WT v. *Casq2*$^{-/-}$), hash indicates significant difference at the alpha = .05 level between tests for the same genotypes (Student's t-Test), and diamond indicates significance at the alpha = .007 level (MANOVA, multiple comparisons Tukey HSD for the PXT_m and GXT_m of obese v. *Casq2*$^{-/-}$).

doi:10.1371/journal.pone.0148010.g003

Similar to VO_{2max} data, only the GXT_m provided a significant decrease in time until exhaustion in the *Casq2*$^{-/-}$ and obese mice (alpha = .007; MANOVA, Tukey HSD Multiple Comparisons; p = .006, *Casq2*$^{-/-}$; p = .001, obese; Fig 4A). Maximum run speed was also only significantly reduced with the GXT_m, but not the PXT_m, in both dysfunctional models (alpha = .007; MANOVA, Tukey HSD Multiple Comparisons; p = .006, *Casq2*$^{-/-}$; p = .001, obese; Fig 5C). In the PXT_m, significant reductions in time until exhaustion and run speed were not observed in the dysfunctional groups (Fig 4A and Fig 5C). This indicated that the PXT_m did not induce sufficient cardiovascular stress to allow for the detection of impaired CVF in established models of cardiac insufficiency. The results of the ANCOVA tests with weight being used as a covariant for the calorimetry data (VO_2 and other variables) are also described and discussed in S3 Text.

The *Casq2*$^{-/-}$ mice, a known model of cardiac insufficiency [23] ran longer than healthy WT controls during the PXT_m (Fig 4A, S4 Text). This was not seen with the GXT_m though; as the WT performed the longest and ran the fastest (Fig 5A). Considering that it has already been established that the *Casq2*$^{-/-}$ model phenocopies humans with CASQ2 mutations [23], and that humans with CASQ2 mutations can be diagnosed with graded maximal exercise tests, we performed further studies investigating the performance of the *Casq2*$^{-/-}$ mice [23, 86–88] (S4 Text, and S8 Table). We concluded that *Casq2*$^{-/-}$ had superior performance on the PXT_m, but impaired performance on the GXT_m, because the PXT_m did not provide enough stress to elicit impaired CVF in these mice. That conclusion was in line with the original findings that showed running time until exhaustion does not change between WT and *Casq2*$^{-/-}$ mice when the maximal exercise test has a set inclination. It should be noted, that both catecholamine challenge and exhaustive

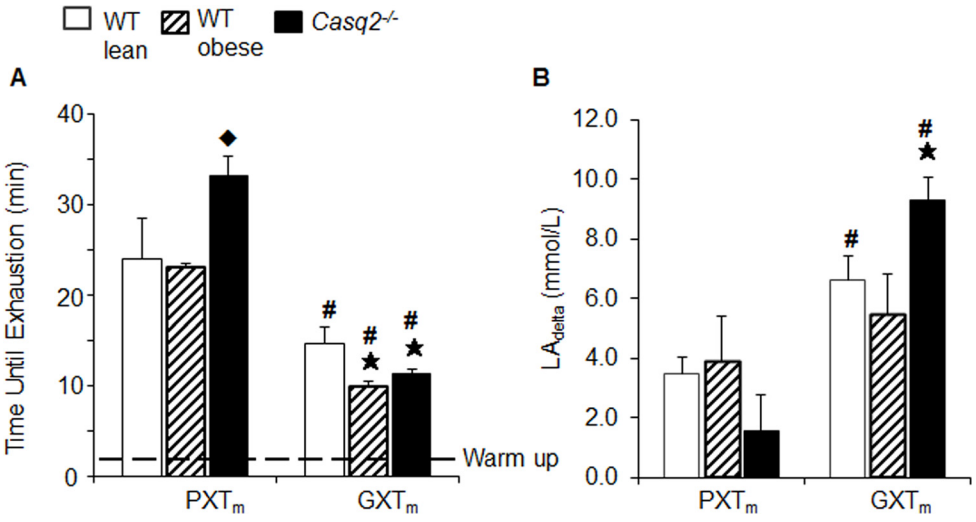

Fig 4. Time until exhaustion at true VO_{2max} is confirmed by increases in lactate concentrations and demonstrates impaired cardiovascular fitness with the GXT_m, but not the PXT_m. (A) Time until exhaustion derived from VO_2 kinetics in same groups of mice described in Fig 3. The dashed line shows the time used for warm up. (B) Change from pre to post test lactate concentration (LA_{delta}) in same group of mice. Bar graphs represent mean ± SD for all but lactate, which is mean ± SEM. Student's t-Test; $p < .05$, WT v. *Casq2*$^{-/-}$.

doi:10.1371/journal.pone.0148010.g004

exercise with ECG monitoring have shown that *Casq2*$^{-/-}$ mice display cardiovascular dysfunction in the form of catecholaminergic polymorphic ventricular tachycardia [23].

The onset of exhaustion is validated in human testing by elevated post-test blood LA (LA_{delta}; LA_{post}-LA_{pre}) concentrations (~8-10mmol/) compared to baseline [4, 55, 74]. We observed significant increases in LA_{delta} using the GXT_m compared to the PXT_m in WT and *Casq2*$^{-/-}$ groups. With the GXT_m, *Casq2*$^{-/-}$ mice had significantly greater LA_{delta} compared to WT; however, with the PXT_m, this parameter was decreased compared to controls (Fig 4B, S9 Table). In humans with myocardial ischemia, a hallmark response to a GXT_h is a significant increase in circulating blood LA concentrations compared to healthy subjects [89]. Thus, this response was replicated with the GXT_m in the genetic model of cardiac insufficiency (9.32 ±1.53mmol/L, *Casq2*$^{-/-}$ v. 6.63 ±17mmol/L; WT; Student's t-Test, alpha = .05; Fig 4B, S9 Table).

RER kinetics indicated that PXT_m could not clearly determine AT to assess CVF; however, RER kinetics from all single GXT_m was capable of determining AT in healthy and dysfunctional models. No significant difference was found between the mean relative AT in functional and dysfunctional mice using the PXT_m (alpha = .007, MANOVA, Tukey HSD Multiple Comparisons, $p = .002$; WT v. *Casq2*$^{-/-}$ during GXT_m; Fig 5B). With the GXT_m, *Casq2*$^{-/-}$ mice also had significantly higher relative ATs compared to WT controls. Thus, with GXT_m, AT was lower in dysfunctional mice; a finding similar to those from human research looking at AT in patients with cardiac disease above functional class I (S5 Text, [90]). Together, these results demonstrated that the GXT_m, like the GXT_h [4, 72, 74, 89, 91], was able to simultaneously elicit exhaustive efforts, true VO_{2max}, and shift to anaerobic metabolism [4, 72, 74, 89, 91].

Fuel utilization differs between healthy mice and models of cardiovascular dysfunction during exercise testing

We determined values of carbohydrate or fat oxidation during both the PXT_m and GXT_m by converting RER values recording during testing into their respective fat and carbohydrate oxidation values (Fig 6, S3 Table).

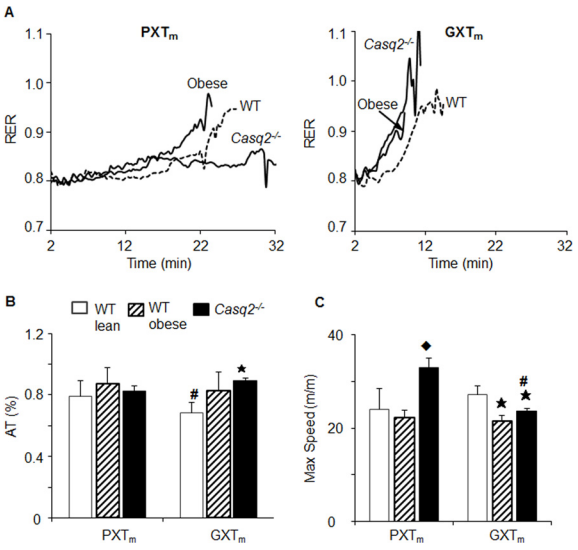

Fig 5. Anaerobic threshold and maximum speed assess dysfunction in mice with the GXT_m, but not the PXT_m. (A) Average RER kinetics from same from WT (dashed line), *Casq2*$^{-/-}$ (solid thick line), and obese (solid line) mice performed the PXT_m and GXT_m. (B) AT was reported as %AT, a time point where AT occurred/total test time in mouse groups (Fig 3). (C) Maximum speed achieved on test (m/m). For all measures, asterisks indicates significance at the alpha = .007 level (MANOVA, multiple comparisons Tukey HSD for the PXT_m and GXT_m of WT v. obese and WT v. *Casq2*$^{-/-}$), hash indicates significant difference at the alpha = .05 level between tests for the same genotype (Student's t-Test), and diamond indicates significance at the alpha = .007 level (mean ± SD, MANOVA, multiple comparisons Tukey HSD for the PXT_m and GXT_m of obese v. *Casq2*$^{-/-}$).

doi:10.1371/journal.pone.0148010.g005

With PXT_m there were multiple crossover points from fat to carbohydrate oxidation during tests, making it difficult to identify a single crossover point. Unlike the PXT_m, the GXT_m allowed for identification of an accurate crossover point in all single tests. In humans, crossover

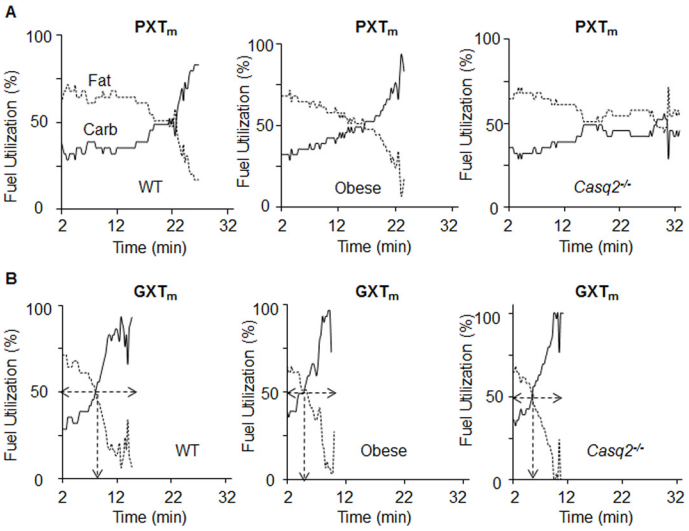

Fig 6. Carbohydrate and fat oxidation kinetics can be used to identify the crossover point in the GXT_m, but not the PXT_m. Averaged fuel utilization kinetics in WT (n = 7), obese (n = 11), and *Casq2*$^{-/-}$ (n = 4) mice. Fat (dashed line) and carbohydrate (Carb, solid line)) oxidation were derived from RER as described in S3 Table during the PXT_m (A) and GXT_m tests (B). In GXT_m tests, the arrow indicates crossover, the point at which carbohydrate and fat oxidation intersect (dashed arrows).

doi:10.1371/journal.pone.0148010.g006

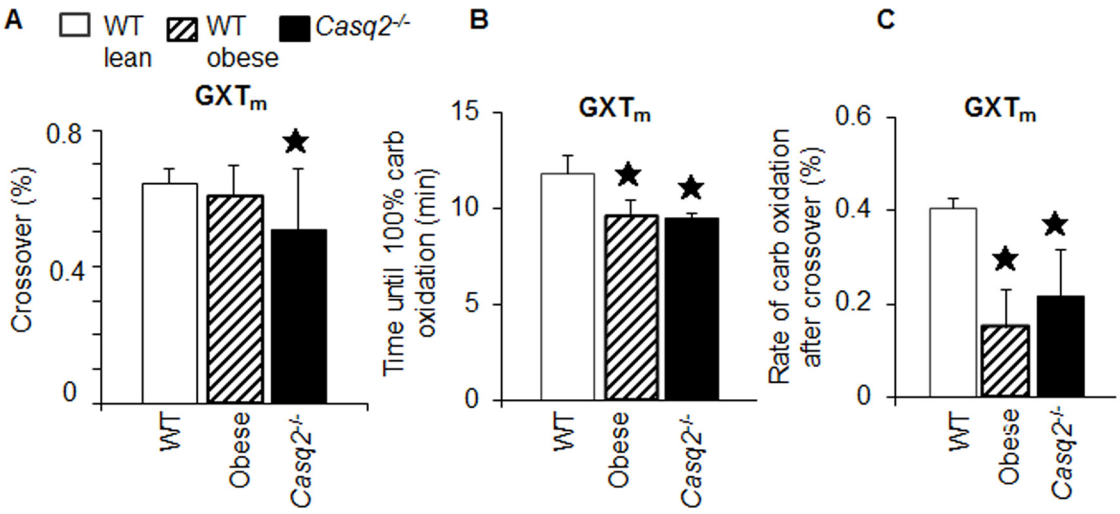

Fig 7. Carbohydrate and fat oxidation parameters from the GXT_m, but not the PXT_m, can be used to identify impaired cardiovascular fitness in dysfunctional models. (A) Fuel utilization kinetics (Fig 6B) from the GXT_m were used to quantify the percent of the test at which the crossover point was achieved relative to total time of test (% of test time at which crossover is achieved is the minute crossover occurred divided by total test time and multiplied by 100). Asterisk indicates significance at the alpha = .007 level (MANOVA, multiple comparisons Tukey HSD for the GXT_m). (B) Time until 100% carbohydrate oxidation. Asterisks show significant difference between dysfunctional v. WT groups, (Student's T-test, GXT_m for WT v. obese and WT v. *Casq2*$^{-/-}$). (C) Rate of carbohydrate oxidation after crossover in all mouse groups. This rate is determined by dividing time after crossover by total time of test (100%) (Student's T-test for the GXT_m for WT v. obese and WT v. *Casq2*$^{-/-}$. Bar graphs represent mean ± SD).

doi:10.1371/journal.pone.0148010.g007

occurs at between 60–80% of aerobic power [71]. We observed crossover in this range with all genotypes on the GXT_m. Specifically, it occurred sooner in the *Casq2*$^{-/-}$ compared to WT controls (Student's T-test, $p < .05$; WT v. *Casq2*$^{-/-}$; Fig 7A). Time to 100% carbohydrate oxidation during GXT_m testing was significantly shorter in dysfunctional animals compared to WT mice (Student's T-test, $p < .05$; WT v. *Casq2*$^{-/-}$, $p < .05$; WT v. obese; Fig 7B) and the rate of carbohydrate oxidation after crossover was decreased (Student's T-test, $p < .05$; WT v. *Casq2*$^{-/-}$, $p < .05$; WT v. obese; Fig 7C). Together these results indicated that substrate utilization parameters from the GXT_m could be used to identify the crossover point and determine fuel use during aerobic and anaerobic stress conditions.

Discussion

GXT design considerations

For over 50 years, exercise testing has served as an established and validated method for diagnostic and prognostic assessment of CVF in the clinical setting [9]. Physicians and exercise physiologists value the use of the GXT_h for induction of physiological stress [92] to the cardiopulmonary system in a controlled environment with simultaneous monitoring of myocardial oxygen demands [93], biochemical [94], and metabolic [71] responses. Furthermore, it is a validated method of evaluating the status of patients with cardiovascular and pulmonary disease [2]. Established GXT_h tests involve gradual increases in work output over multi-stage increases in speed and inclination [95] (Table 1). When generating the GXT_m, we applied the same principle design and used staged increases in speed and inclination, as well as similar end point criteria for a positive test (S4 Table). Since both human and mouse exercise tests analyze VCO_2, VO_2, and RER through the use of indirect calorimetry; an attempt was made to utilize information generated from metabolic data while acknowledging the differences which will always persist between species.

The available equipment for exercise test in mice and human is another factor that was considered during development of the GXT_m. In human tests, VCO_2 and VO_2 are measured each breath, whereas with mice, this information is generated from the gas exchange occurring inside the metabolic chamber which encloses the treadmill mice run on. Without the ability to calculate single breath values in running mice, the ventilatory rate cannot be calculated. Furthermore, the diffusion of gas from the chamber to the sensor elicits an approximate one-minute lag in mice testing. Thus, this must be accounted for data interpretation and analysis. Given that some of the biggest differences between mouse and human cardiac physiology occur in respect to heart rate, size, and oxygen requirements (reviewed in [60]), we recognized it was essential to rely on variables which were normalized to animal size and oxygen rates (RER, fuel substrate oxidation) to focus the similarities of comparative exercise physiology of mice and men.

Another difference between human and mouse testing included test termination. A shock grid wills maximal exertion attempts in mice; where as in humans, they run at their own volition. Accordingly, appropriate acclimation to treadmill testing must be completed in mice to reduce the physiological and psychological stress potentially associated with their initial introduction to shock. Outside of these limitations though, the adjustments we made to stage length and intensity, and the alterations we made to account for perpetual differences between mice and humans, allowed us to develop a method of exercise testing for mice that induced true VO_{2max} and generated a set of variables that were comparable to data acquired from human testing (AT, crossover, $Lactate_{delta}$)

The value of determining anaerobic threshold in mouse exercise testing

The field of exercise physiology has established that the relationship between VO_2 and work rate diminishes in tests lasting less than 6 minutes or greater than 12 minutes [2]. Furthermore, they have shown that tests lasting over 12 minutes provide data that is impacted by skeletal muscle fatigue and orthopedic issues [2]. The PXT_m was composed of a large volume of submaximal work. During this exercise intensity, there is a decreased demand for oxygen and a reduction in the redistribution of blood from inactive to active tissues. This submaximal intensity delays time until maximum cardiac output, ventilation, and VO_{2max} [63]. In the $PXT_{m,}$ this type of scenario occurs, as the cardiovascular system is not maximally stressed until later stages of the test. Accordingly, this test can be considered too long to specifically stress the cardiorespiratory system and its ability to withstand metabolic stress. Our data showed that the PXT_m is likely a superior test for assessing aerobic exercise capacity and aerobic endurance; whereas, the GXT_m is superior for assessing CVF.

A long test can be problematic if a researcher wants to report parameters beyond maximum run speed or duration, such as AT and crossover, to determine the cardiometabolic phenotype of a mouse. This limitation was observed in classic PXT_m, as it was incapable of producing RER kinetics to determine AT. Typically AT can be identified by a nonlinear increase in minute ventilation [92]; however, this is not feasible for most researchers to calculate in mouse models during exercise [96]. In our GXT_m test we were able to use abrupt exponential increases in RER to determine the point at which AT occurred in both WT and dysfunctional models. These AT values derived in our GXT_m provided a sensitive measure for determining CVF in mice. Clinically, AT has been used in patients with cardiorespiratory disease to assess exercise tolerance [85]; however, the ability to derive AT from an exercise test has additional applications such as evaluating endurance performance, exercise prescription, and determining the effects of drugs on exercise tolerance (reviewed in [97]). Thus, the ability of the GXT_m to derive AT values highlighted its capability to generate novel noninvasive diagnostics and quantitative assessments of CVF in various mouse models.

Metabolic crossover, an old human metabolic parameter with new applications in mouse testing

We found the GXT_m was capable of predicting AT based off of RER values, but it was also capable of determining the specific point of crossover from predominate lipid to carbohydrate oxidation during testing. This shift in fuel substrate utilization, known as the crossover concept [98], demonstrates that as relative VO_2 and power output increase, there is a shift to predominate carbohydrate utilization. Thus, the shift from predominant of lipid oxidation to an increased dependence on muscle glycogen and blood glucose substrates [98] is intensity driven. This concept had been well established with methods such as radio-tracers, tissue metabolite sampling, stable isotopes, and indirect calorimetry in mammals and man [99] (reviewed in [98]). With the GXT_m, the use of glycogen and glucose oxidation increased exponentially with exercise intensity and, therefore, allowed for crossover determination (Figs 6 and 7). It should be noted, as demonstrated in the data of a single WT mouse (Fig 2), that AT and crossover did not occur simultaneously in the GXT_m testing and were both difficult to interpret in PXT_m testing. The effect seen in the GXT_m could potentially be due to pyruvate dehydrogenase (PDH) mediated LA accumulation and aerobic substrate oxidation [100]. In working muscles, transformation of the pyruvate dehydrogenase complex (PDHc) to the active form (PDHa) is complete at approximately 80% VO_{2max} [101]; however, crossover occurs at approximately 65% percent of VO_{2max} [71]. With the GXT_m, both crossover and AT were found around these approximations, with crossover occurring at 62–75% and AT occurring between 68–87% in mice. Regardless of these differences, the crossover obtained in our study with established model cardiovascular dysfunction was similar; yet significantly different than the healthy WT controls.

Standardized methods for the functional assessment of cardiovascular fitness in mice

Without a gold standard *in vivo* exercise assay, reported data become both unreliable and difficult to reproduce between researchers. Previous mouse exercise assays have not considered both components of human exercise testing and the limitations of exercise testing in mice. However, as we have shown, certain testing conditions in mice allow for the reporting of cardio-metabolic parameters previously only reported in human testing. With the appropriate considerations to test design and differences between mouse and human physiology, tests like the GXT_m can serve as noninvasive, cost effective, methods to assess the cardio-metabolic phenotype of mice. Our data showed that the GXT_m was able to consistently provide data about the CVF of various models, and thus, could be used in the future to examine the effects of various treatments and therapeutics.

Alternative cardiac challenges using echocardiography [102] and cardiac magnetic resonance imaging ($_c$MRI) [103] are popularized protocols to stress and test the cardiovascular system in mouse models; however, they are expensive and require animals to be anesthetized. Anesthesia prevents animal heart rates from achieving the true physiological responses to reagents and compromises cardiac output, a measure of blood being pumped by the heart per minute. Unlike these procedures, exercise assays have been shown to elicit a 2-fold increase in cardiac output [104] while avoiding limitations of anesthesia. Appropriate exercise testing and exercise prescription clearly have a place in the assessment and management of cardiovascular disease. Accordingly, exercise testing and prescription could carry a similar weight in mouse cardiovascular research if there was more standardization amongs the methods used to determine CVF in mice. If research done on mice is aimed at elucidating mechanisms of disease and therapies; then it is critical to apply tests that specifically test the CVF of mice when assessing cardio-metabolic function.

Supporting Information

S1 File. Contains supporting tables, figures, and notes.
(DOCX)

Acknowledgments

We thank Dr. Alexander Lucas, Dr. Brian Focht, Grant Foglesong, and Shawn Flanagan their suggestions during manuscript generation.

Author Contributions

Conceived and designed the experiments: JMP RAL OPS. Performed the experiments: JMP RAL OPS. Analyzed the data: JMP VJH. Contributed reagents/materials/analysis tools: AK SKM MP JMW. Wrote the paper: JMP OZ.

References

1. Poirier P, Giles TD, Bray GA, Hong Y, Stern JS, Pi-Sunyer FX, et al. Obesity and cardiovascular disease: pathophysiology, evaluation, and effect of weight loss: an update of the 1997 American Heart Association Scientific Statement on Obesity and Heart Disease from the Obesity Committee of the Council on Nutrition, Physical Activity, and Metabolism. Circulation. 2006; 113(6):898–918. doi: 10.1161/CIRCULATIONAHA.106.171016 PMID: 16380542.
2. Balady GJ, Arena R, Sietsema K, Myers J, Coke L, Fletcher GF, et al. Clinician's Guide to cardiopulmonary exercise testing in adults: a scientific statement from the American Heart Association. Circulation. 2010; 122 (2):191–225. Epub 2010/06/30. doi: 10.1161/CIR.0b013e3181e52e69 PMID: 20585013.
3. Ehrman JK, American College of Sports Medicine. ACSM's resource manual for Guidelines for exercise testing and prescription. 6th ed. Philadelphia: Wolters Kluwer Health/Lippincott Williams & Wilkins; 2010. xxiv, 868 p. p.
4. Pescatello LS, American College of Sports Medicine. ACSM's guidelines for exercise testing and prescription. 9th ed. Philadelphia: Wolters Kluwer/Lippincott Williams & Wilkins Health; 2014. xxiv, 456 p. p.
5. Bruce RA, Kusumi F, Hosmer D. Maximal oxygen intake and nomographic assessment of functional aerobic impairment in cardiovascular disease. American heart journal. 1973; 85(4):546–62. PMID: 4632004.
6. Mead WF. Maximal exercise testing—Bruce protocol. The Journal of family practice. 1979; 9(3):479–90. PMID: 479779.
7. Kodama S, Saito K, Tanaka S, Maki M, Yachi Y, Asumi M, et al. Cardiorespiratory fitness as a quantitative predictor of all-cause mortality and cardiovascular events in healthy men and women: a meta-analysis. JAMA: the journal of the American Medical Association. 2009; 301(19):2024–35. doi: 10.1001/jama.2009.681 PMID: 19454641.
8. Gupta S, Rohatgi A, Ayers CR, Willis BL, Haskell WL, Khera A, et al. Cardiorespiratory fitness and classification of risk of cardiovascular disease mortality. Circulation. 2011; 123(13):1377–83. doi: 10.1161/CIRCULATIONAHA.110.003236 PMID: 21422392; PubMed Central PMCID: PMC3926656.
9. Swain DP, American College of Sports Medicine., American College of Sports Medicine. ACSM's resource manual for guidelines for exercise testing and prescription. 7th ed. Philadelphia: Wolters Kluwer Health/Lippincott Williams & Wilkins; 2014. xv, 862 p. p.
10. Chu G, Haghighi K, Kranias EG. From mouse to man: understanding heart failure through genetically altered mouse models. Journal of cardiac failure. 2002; 8(6 Suppl):S432–49. doi: 10.1054/jcaf.2002.129284 PMID: 12555156.
11. Jawien J, Nastalek P, Korbut R. Mouse models of experimental atherosclerosis. Journal of physiology and pharmacology: an official journal of the Polish Physiological Society. 2004; 55(3):503–17. PMID: 15381823.
12. Russell LK, Finck BN, Kelly DP. Mouse models of mitochondrial dysfunction and heart failure. Journal of molecular and cellular cardiology. 2005; 38(1):81–91. doi: 10.1016/j.yjmcc.2004.10.010 PMID: 15623424.
13. Breckenridge R. Heart failure and mouse models. Disease models & mechanisms. 2010; 3(3–4):138–43. doi: 10.1242/dmm.005017 PMID: 20212081.
14. Fiedler LR, Maifoshie E, Schneider MD. Mouse models of heart failure: cell signaling and cell survival. Current topics in developmental biology. 2014; 109:171–247. doi: 10.1016/B978-0-12-397920-9.00002–0 PMID: 24947238.
15. Piedrahita JA, Zhang SH, Hagaman JR, Oliver PM, Maeda N. Generation of mice carrying a mutant apolipoprotein E gene inactivated by gene targeting in embryonic stem cells. Proceedings of the National Academy

of Sciences of the United States of America. 1992; 89(10):4471–5. PMID: 1584779; PubMed Central PMCID: PMC49104.

16. Shesely EG, Maeda N, Kim HS, Desai KM, Krege JH, Laubach VE, et al. Elevated blood pressures in mice lacking endothelial nitric oxide synthase. Proceedings of the National Academy of Sciences of the United States of America. 1996; 93(23):13176–81. PMID: 8917564; PubMed Central PMCID: PMC24066.

17. Li Y, Gilbert TR, Matsumoto AH, Shi W. Effect of aging on fatty streak formation in a diet-induced mouse model of atherosclerosis. Journal of vascular research. 2008; 45(3):205–10. doi: 10.1159/000112133 PMID: 18063868; PubMed Central PMCID: PMC2373261.

18. Aoyagi T, Higa JK, Aoyagi H, Yorichika N, Shimada BK, Matsui T. Cardiac mTOR rescues the detrimental effects of diet-induced obesity in the heart after ischemia-reperfusion. American journal of physiology Heart and circulatory physiology. 2015; 308(12):H1530–9. doi: 10.1152/ajpheart.00008.2015 PMID: 25888508; PubMed Central PMCID: PMC4469881.

19. Winzell MS, Ahren B. The high-fat diet-fed mouse: a model for studying mechanisms and treatment of impaired glucose tolerance and type 2 diabetes. Diabetes. 2004; 53 Suppl 3:S215–9. PMID: 15561913.

20. Zeng H, Vaka VR, He X, Booz GW, Chen JX. High-fat diet induces cardiac remodelling and dysfunction: assessment of the role played by SIRT3 loss. Journal of cellular and molecular medicine. 2015. doi: 10.1111/jcmm.12556 PMID: 25782072.

21. Kubota T, Kubota N, Kumagai H, Yamaguchi S, Kozono H, Takahashi T, et al. Impaired insulin signaling in endothelial cells reduces insulin-induced glucose uptake by skeletal muscle. Cell metabolism. 2011; 13 (3):294–307. doi: 10.1016/j.cmet.2011.01.018 PMID: 21356519.

22. Barrett EJ, Eggleston EM, Inyard AC, Wang H, Li G, Chai W, et al. The vascular actions of insulin control its delivery to muscle and regulate the rate-limiting step in skeletal muscle insulin action. Diabetologia. 2009; 52(5):752–64. doi: 10.1007/s00125-009-1313-z PMID: 19283361; PubMed Central PMCID: PMC2704146.

23. Knollmann BC, Chopra N, Hlaing T, Akin B, Yang T, Ettensohn K, et al. Casq2 deletion causes sarcoplasmic reticulum volume increase, premature Ca2+ release, and catecholaminergic polymorphic ventricular tachycardia. The Journal of clinical investigation. 2006; 116(9):2510–20. Epub 2006/08/26. doi: 10.1172/JCI29128 PMID: 16932808; PubMed Central PMCID: PMC1551934.

24. Francis J, Sankar V, Nair VK, Priori SG. Catecholaminergic polymorphic ventricular tachycardia. Heart rhythm: the official journal of the Heart Rhythm Society. 2005; 2(5):550–4. doi: 10.1016/j.hrthm.2005.01.024 PMID: 15840485.

25. Postma AV, Denjoy I, Hoorntje TM, Lupoglazoff JM, Da Costa A, Sebillon P, et al. Absence of calsequestrin 2 causes severe forms of catecholaminergic polymorphic ventricular tachycardia. Circulation research. 2002; 91(8):e21–6. PMID: 12386154.

26. Abdurrachim D, Luiken JJ, Nicolay K, Glatz JF, Prompers JJ, Nabben M. Good and bad consequences of altered fatty acid metabolism in heart failure: Evidence from mouse models. Cardiovascular research. 2015. doi: 10.1093/cvr/cvv105 PMID: 25765936.

27. Allen JM, Berg Miller ME, Pence BD, Whitlock K, Nehra V, Gaskins HR, et al. Voluntary and forced exercise differentially alter the gut microbiome in C57BL/6J mice. Journal of applied physiology. 2015: jap.01077.2014. Epub 2015/02/14. doi: 10.1152/japplphysiol.01077.2014 PMID: 25678701.

28. Aoi W, Ogaya Y, Takami M, Konishi T, Sauchi Y, Park EY, et al. Glutathione supplementation suppresses muscle fatigue induced by prolonged exercise via improved aerobic metabolism. Journal of the International Society of Sports Nutrition. 2015; 12:7. Epub 2015/02/17. doi: 10.1186/s12970-015-0067-x PMID: 25685110; PubMed Central PMCID: PMCPmc4328900.

29. Appukutty M, Ramasamy K, Rajan S, Vellasamy S, Ramasamy R, Radhakrishnan AK. Effect of orally administered soy milk fermented with Lactobacillus plantarum LAB12 and physical exercise on murine immune responses. Beneficial microbes. 2015:1–6. Epub 2015/02/19. doi: 10.3920/bm2014.0129 PMID: 25691103.

30. Aschar-Sobbi R, Izaddoustdar F, Korogyi AS, Wang Q, Farman GP, Yang F, et al. Increased atrial arrhythmia susceptibility induced by intense endurance exercise in mice requires TNFalpha. Nature communications. 2015; 6:6018. Epub 2015/01/20. doi: 10.1038/ncomms7018 PMID: 25598495.

31. Borsting Jordy A, Kraakman MJ, Gardner T, Estevez E, Kammoun HL, Weir JM, et al. Analysis of the liver lipidome reveals insights into the protective effect of exercise on high fat diet induced hepatosteatosis in mice. American journal of physiology Endocrinology and metabolism. 2015: Epub 2015/02/26. doi: 10.1152/ajpendo.00547.2014 PMID: 25714675.

32. Cho J, Shin MK, Kim D, Lee I, Kim S, Kang H. Treadmill Running Reverses Cognitive Declines due to Alzheimer's Disease. Medicine and science in sports and exercise. 2015. Epub 2015/01/13. doi: 10.1249/mss.0000000000000612 PMID: 25574797.

33. Fentz J, Kjobsted R, Birk JB, Jordy AB, Jeppesen J, Thorsen K, et al. AMPKalpha is critical for enhancing skeletal muscle fatty acid utilization during in vivo exercise in mice. FASEB journal: official publication of the Federation of American Societies for Experimental Biology. 2015. Epub 2015/01/23. doi: 10.1096/fj.14-266650 PMID: 25609422.

34. Garcia-Pelagio KP, Muriel J, O'Neill A, Desmond PF, Lovering RM, Lund L, et al. Myopathic changes in murine skeletal muscle lacking synemin. American journal of physiology Cell physiology. 2015; 308(6):

C448–62. Epub 2015/01/09. doi: 10.1152/ajpcell.00331.2014 PMID: 25567810; PubMed Central PMCID: PMCPmc4360028.

35. Giacomello E, Quarta M, Paolini C, Squecco R, Fusco P, Toniolo L, et al. Deletion of small ankyrin 1 (sAnk1) isoforms results in structural and functional alterations in aging skeletal muscle fibers. American journal of physiology Cell physiology. 2015; 308(2):C123–38. Epub 2014/10/31. doi: 10.1152/ajpcell.00090.2014 PMID: 25354526.

36. Kadoguchi T, Kinugawa S, Takada S, Fukushima A, Furihata T, Homma T, et al. Angiotensin II can directly induce mitochondrial dysfunction, decrease oxidative fibre number and induce atrophy in mouse hindlimb skeletal muscle. Experimental physiology. 2015; 100(3):312–22. Epub 2015/01/13. doi: 10.1113/expphysiol.2014.084095 PMID: 25580531.

37. Kim DS, Cha HN, Jo HJ, Song IH, Baek SH, Dan JM, et al. TLR2 deficiency attenuates skeletal muscle atrophy in mice. Biochemical and biophysical research communications. 2015. Epub 2015/03/10. doi: 10.1016/j.bbrc.2015.02.144 PMID: 25749338.

38. Knudsen JG, Bienso RS, Hassing HA, Jakobsen AH, Pilegaard H. Exercise-induced regulation of key factors in substrate choice and gluconeogenesis in mouse liver. Molecular and cellular biochemistry. 2015. Epub 2015/02/24. doi: 10.1007/s11010-015-2351-0 PMID: 25702176.

39. Lin TW, Shih YH, Chen SJ, Lien CH, Chang CY, Huang TY, et al. Running exercise delays neurodegeneration in amygdala and hippocampus of Alzheimer's disease (APP/PS1) transgenic mice. Neurobiology of learning and memory. 2015; 118:189–97. Epub 2014/12/30. doi: 10.1016/j.nlm.2014.12.005 PMID: 25543023.

40. MacPherson RE, Huber JS, Frendo-Cumbo S, Simpson JA, Wright DC. Adipose Tissue Insulin Action and IL-6 Signaling following Exercise in Obese Mice. Medicine and science in sports and exercise. 2015. Epub 2015/03/19. doi: 10.1249/mss.0000000000000660 PMID: 25785928.

41. Marchon C, de Marco Ornelas E, da Silva Viegas KA, Lacchini S, de Souza RR, Fonseca FL, et al. Effects of moderate exercise on the biochemical, physiological, morphological and functional parameters of the aorta in the presence of estrogen deprivation and dyslipidemia: an experimental model. Cellular physiology and biochemistry: international journal of experimental cellular physiology, biochemistry, and pharmacology. 2015; 35(1):397–405. Epub 2015/01/17. doi: 10.1159/000369705 PMID: 25591780.

42. Pate KM, Sherk VD, Carpenter RD, Weaver M, Crapo S, Gally F, et al. The beneficial effects of exercise on cartilage are lost in mice with reduced levels of ECSOD in tissues. Journal of applied physiology. 2015; 118(6):760–7. Epub 2015/01/17. doi: 10.1152/japplphysiol.00112.2014 PMID: 25593283.

43. Piguet AC, Saran U, Simillion C, Keller I, Terracciano L, Reeves HL, et al. Regular exercise decreases liver tumors development in hepatocyte-specific PTEN-deficient mice independently of steatosis. Journal of hepatology. 2015. Epub 2015/01/28. doi: 10.1016/j.jhep.2015.01.017 PMID: 25623824.

44. Pincu Y, Linden MA, Zou K, Baynard T, Boppart MD. The effects of high fat diet and moderate exercise on TGFbeta1 and collagen deposition in mouse skeletal muscle. Cytokine. 2015; 73(1):23–9. Epub 2015/02/18. doi: 10.1016/j.cyto.2015.01.013 PMID: 25689619.

45. Rank MM, Flynn JR, Battistuzzo CR, Galea MP, Callister R, Callister RJ. Functional changes in deep dorsal horn interneurons following spinal cord injury are enhanced with different durations of exercise training. The Journal of physiology. 2015; 593(1):331–45. Epub 2015/01/06. doi: 10.1113/jphysiol.2014.282640 PMID: 25556804; PubMed Central PMCID: PMCPmc4293071.

46. Sashindranath M, Daglas M, Medcalf RL. Evaluation of gait impairment in mice subjected to craniotomy and traumatic brain injury. Behavioural brain research. 2015; 286:33–8. Epub 2015/02/28. doi: 10.1016/j.bbr.2015.02.038 PMID: 25721743.

47. Sommer W, Knofel AK, Izykowski N, Oldhafer F, Avsar M, Jonigk D, et al. Physical exercise reduces transplant arteriosclerosis in a mouse aorta transplantation model. The Journal of thoracic and cardiovascular surgery. 2015; 149(1):330–7. Epub 2014/12/20. doi: 10.1016/j.jtcvs.2014.10.029 PMID: 25524687.

48. Uchiyama M, Jin X, Yin E, Shimokawa T, Niimi M. Treadmill exercise induces murine cardiac allograft survival and generates regulatory T cell. Transplant international: official journal of the European Society for Organ Transplantation. 2015; 28(3):352–62. Epub 2014/11/20. doi: 10.1111/tri.12491 PMID: 25406375.

49. Vogel J, Kruse C, Zhang M, Schroder K. Nox4 supports proper capillary growth in exercise and retina neovascularization. The Journal of physiology. 2015. Epub 2015/02/06. doi: 10.1113/jphysiol.2014.284901 PMID: 25652847.

50. Wallace IJ, Gupta S, Sankaran J, Demes B, Judex S. Bone shaft bending strength index is unaffected by exercise and unloading in mice. Journal of anatomy. 2015; 226(3):224–8. Epub 2015/02/04. doi: 10.1111/joa.12277 PMID: 25645569.

51. Wallace IJ, Judex S, Demes B. Effects of load-bearing exercise on skeletal structure and mechanics differ between outbred populations of mice. Bone. 2015; 72:1–8. Epub 2014/12/03. doi: 10.1016/j.bone.2014.11.013 PMID: 25460574.

52. Wood LK, Brooks SV. Ten weeks of treadmill running decreases stiffness and increases collagen turnover in tendons of old mice. Journal of orthopaedic research: official publication of the Orthopaedic Research Society. 2015. Epub 2015/02/03. doi: 10.1002/jor.22824 PMID: 25640809.

53. Zheng DM, Bian Z, Furuya N, Oliva Trejo JA, Takeda-Ezaki M, Takahashi K, et al. A treadmill exercise reactivates the signaling of the mammalian target of rapamycin (mTor) in the skeletal muscles of starved mice. Biochemical and biophysical research communications. 2015; 456(1):519–26. Epub 2014/12/09. doi: 10.1016/j.bbrc.2014.11.118 PMID: 25485704.

54. Zou K, Huntsman HD, Carmen Valero M, Adams J, Skelton J, De Lisio M, et al. Mesenchymal stem cells augment the adaptive response to eccentric exercise. Medicine and science in sports and exercise. 2015; 47(2):315–25. Epub 2014/06/07. doi: 10.1249/mss.0000000000000405 PMID: 24905768.

55. Booth FW, Laye MJ, Spangenburg EE. Gold standards for scientists who are conducting animal-based exercise studies. Journal of applied physiology. 2010; 108(1):219–21. doi: 10.1152/japplphysiol.00125.2009 PMID: 19574508.

56. Ostler JE, Maurya SK, Dials J, Roof SR, Devor ST, Ziolo MT, et al. Effects of insulin resistance on skeletal muscle growth and exercise capacity in type 2 diabetic mouse models. American journal of physiology Endocrinology and metabolism. 2014; 306(6):E592–605. Epub 2014/01/16. doi: 10.1152/ajpendo.00277.2013 PMID: 24425761; PubMed Central PMCID: PMC3948983.

57. Hernandez OM, Szczesna-Cordary D, Knollmann BC, Miller T, Bell M, Zhao J, et al. F110I and R278C troponin T mutations that cause familial hypertrophic cardiomyopathy affect muscle contraction in transgenic mice and reconstituted human cardiac fibers. The Journal of biological chemistry. 2005; 280(44):37183–94. Epub 2005/08/24. doi: 10.1074/jbc.M508114200 PMID: 16115869.

58. Calvo JA, Daniels TG, Wang X, Paul A, Lin J, Spiegelman BM, et al. Muscle-specific expression of PPARgamma coactivator-1alpha improves exercise performance and increases peak oxygen uptake. Journal of applied physiology. 2008; 104(5):1304–12. doi: 10.1152/japplphysiol.01231.2007 PMID: 18239076.

59. Fletcher GF, Ades PA, Kligfield P, Arena R, Balady GJ, Bittner VA, et al. Exercise standards for testing and training: a scientific statement from the American Heart Association. Circulation. 2013; 128(8):873–934. doi: 10.1161/CIR.0b013e31829b5b44 PMID: 23877260.

60. Doevendans PA, Daemen MJ, de Muinck ED, Smits JF. Cardiovascular phenotyping in mice. Cardiovascular research. 1998; 39(1):34–49. PMID: 9764188.

61. Wessels A, Sedmera D. Developmental anatomy of the heart: a tale of mice and man. Physiological genomics. 2003; 15(3):165–76. doi: 10.1152/physiolgenomics.00033.2003 PMID: 14612588.

62. Pollock ML, Franklin BA, Balady GJ, Chaitman BL, Fleg JL, Fletcher B, et al. AHA Science Advisory. Resistance exercise in individuals with and without cardiovascular disease: benefits, rationale, safety, and prescription: An advisory from the Committee on Exercise, Rehabilitation, and Prevention, Council on Clinical Cardiology, American Heart Association; Position paper endorsed by the American College of Sports Medicine. Circulation. 2000; 101(7):828–33. Epub 2000/02/23. PMID: 10683360.

63. Wisloff U, Helgerud J, Kemi OJ, Ellingsen O. Intensity-controlled treadmill running in rats: VO(2 max) and cardiac hypertrophy. American journal of physiology Heart and circulatory physiology. 2001; 280(3):H1301–10. PMID: 11179077.

64. Henderson KK, Wagner H, Favret F, Britton SL, Koch LG, Wagner PD, et al. Determinants of maximal O(2) uptake in rats selectively bred for endurance running capacity. Journal of applied physiology. 2002; 93(4):1265–74. doi: 10.1152/japplphysiol.00809.2001 PMID: 12235024.

65. Kemi OJ, Loennechen JP, Wisloff U, Ellingsen O. Intensity-controlled treadmill running in mice: cardiac and skeletal muscle hypertrophy. Journal of applied physiology. 2002; 93(4):1301–9. doi: 10.1152/japplphysiol.00231.2002 PMID: 12235029.

66. Fueger PT, Shearer J, Krueger TM, Posey KA, Bracy DP, Heikkinen S, et al. Hexokinase II protein content is a determinant of exercise endurance capacity in the mouse. The Journal of physiology. 2005; 566(Pt 2):533–41. doi: 10.1113/jphysiol.2005.085043 PMID: 15878951; PubMed Central PMCID: PMC1464755.

67. Rezende EL, Garland T Jr, Chappell MA, Malisch JL, Gomes FR. Maximum aerobic performance in lines of Mus selected for high wheel-running activity: effects of selection, oxygen availability and the mini-muscle phenotype. The Journal of experimental biology. 2006; 209(Pt 1):115–27. doi: 10.1242/jeb.01883 PMID: 16354783.

68. Ericsson M, Andersson KB, Amundsen BH, Torp SH, Sjaastad I, Christensen G, et al. High-intensity exercise training in mice with cardiomyocyte-specific disruption of Serca2. Journal of applied physiology. 2010; 108(5):1311–20. doi: 10.1152/japplphysiol.01133.2009 PMID: 20167673.

69. Rocco AB, Levalley JC, Eldridge JA, Marsh SA, Rodgers BD. A novel protocol for assessing exercise performance and dystropathophysiology in the mdx mouse. Muscle & nerve. 2014; 50(4):541–8. doi: 10.1002/mus.24184 PMID: 24449511.

70. Wasserman K. The anaerobic threshold measurement in exercise testing. Clinics in chest medicine. 1984; 5(1):77–88. PMID: 6723245.

71. Brooks GA, Mercier J. Balance of carbohydrate and lipid utilization during exercise: the "crossover" concept. Journal of applied physiology. 1994; 76(6):2253–61. Epub 1994/06/01. PMID: 7928844.

72. Wasserman K. Lactate and related acid base and blood gas changes during constant load and graded exercise. Canadian Medical Association journal. 1967; 96(12):775–83. PMID: 6020874; PubMed Central PMCID: PMC1936113.

73. Myers J. Essentials of cardiopulmonary exercise testing. Champaign, IL: Human Kinetics; 1996. xiii, 177 p. p.

74. Platt C, Houstis N, Rosenzweig A. Using Exercise to Measure and Modify Cardiac Function. Cell metabolism. 2015; 21(2):227–36. doi: 10.1016/j.cmet.2015.01.014 PMID: 25651177; PubMed Central PMCID: PMC4317572.

75. Kalyanasundaram A, Viatchenko-Karpinski S, Belevych AE, Lacombe VA, Hwang HS, Knollmann BC, et al. Functional consequences of stably expressing a mutant calsequestrin (CASQ2D307H) in the CASQ2 null background. American journal of physiology Heart and circulatory physiology. 2012; 302(1):H253–61. doi: 10.1152/ajpheart.00578.2011 PMID: 21984545; PubMed Central PMCID: PMC3334241.

76. Stolen TO, Hoydal MA, Kemi OJ, Catalucci D, Ceci M, Aasum E, et al. Interval training normalizes cardiomyocyte function, diastolic Ca2+ control, and SR Ca2+ release synchronicity in a mouse model of diabetic cardiomyopathy. Circulation research. 2009; 105(6):527–36. Epub 2009/08/15. doi: 10.1161/CIRCRESAHA.109.199810 PMID: 19679837.

77. Ferreira JC, Rolim NP, Bartholomeu JB, Gobatto CA, Kokubun E, Brum PC. Maximal lactate steady state in running mice: effect of exercise training. Clinical and experimental pharmacology & physiology. 2007; 34(8):760–5. doi: 10.1111/j.1440-1681.2007.04635.x PMID: 17600553.

78. Lund J, Hafstad AD, Boardman NT, Rossvoll L, Rolim NP, Ahmed MS, et al. Exercise training promotes cardioprotection through oxygen-sparing action in high fat-fed mice. American journal of physiology Heart and circulatory physiology. 2015; 308(8):H823–9. doi: 10.1152/ajpheart.00734.2014 PMID: 25637547.

79. Han Y, Oshida Y, Li L, Koshinaka K, Fuku N, Yamanouchi K, et al. Effect of voluntary wheel-running on insulin sensitivity and responsiveness in high-fat-fed rats. Endocrine journal. 2001; 48(5):551–5. PMID: 11789559.

80. Podolin DA, Wei Y, Pagliassotti MJ. Effects of a high-fat diet and voluntary wheel running on gluconeogenesis and lipolysis in rats. Journal of applied physiology. 1999; 86(4):1374–80. PMID: 10194225.

81. Rezende EL, Chappell MA, Gomes FR, Malisch JL, Garland T Jr. Maximal metabolic rates during voluntary exercise, forced exercise, and cold exposure in house mice selectively bred for high wheel-running. The Journal of experimental biology. 2005; 208(Pt 12):2447–58. doi: 10.1242/jeb.01631 PMID: 15939783.

82. Rezende EL, Gomes FR, Malisch JL, Chappell MA, Garland T Jr. Maximal oxygen consumption in relation to subordinate traits in lines of house mice selectively bred for high voluntary wheel running. Journal of applied physiology. 2006; 101(2):477–85. doi: 10.1152/japplphysiol.00042.2006 PMID: 16601309.

83. Meek TH, Eisenmann JC, Garland T Jr. Western diet increases wheel running in mice selectively bred for high voluntary wheel running. International journal of obesity. 2010; 34(6):960–9. doi: 10.1038/ijo.2010.25 PMID: 20157317.

84. Bassett DR Jr, Howley ET. Limiting factors for maximum oxygen uptake and determinants of endurance performance. Medicine and science in sports and exercise. 2000; 32(1):70–84. PMID: 10647532.

85. Wasserman K, McIlroy MB. Detecting the Threshold of Anaerobic Metabolism in Cardiac Patients during Exercise. The American journal of cardiology. 1964; 14:844–52. PMID: 14232808.

86. Glukhov AV, Kalyanasundaram A, Lou Q, Hage LT, Hansen BJ, Belevych AE, et al. Calsequestrin 2 deletion causes sinoatrial node dysfunction and atrial arrhythmias associated with altered sarcoplasmic reticulum calcium cycling and degenerative fibrosis within the mouse atrial pacemaker complex1. European heart journal. 2015; 36(11):686–97. doi: 10.1093/eurheartj/eht452 PMID: 24216388; PubMed Central PMCID: PMC4359358.

87. Lerman I, Harrison BC, Freeman K, Hewett TE, Allen DL, Robbins J, et al. Genetic variability in forced and voluntary endurance exercise performance in seven inbred mouse strains. Journal of applied physiology. 2002; 92(6):2245–55. doi: 10.1152/japplphysiol.01045.2001 PMID: 12015333.

88. Courtney SM, Massett MP. Identification of exercise capacity QTL using association mapping in inbred mice. Physiological genomics. 2012; 44(19):948–55. doi: 10.1152/physiolgenomics.00051.2012 PMID: 22911454; PubMed Central PMCID: PMC3472463.

89. Chalmers RJ, Johnson RH, Al Badran RH, Williams BO. Metabolic changes during exercise testing of patients with ischaemic heart disease. European journal of applied physiology and occupational physiology. 1976; 35(4):261–9. PMID: 976253.

90. Wasserman K, Whipp BJ, Koyl SN, Beaver WL. Anaerobic threshold and respiratory gas exchange during exercise. J Appl Physiol. 1973; 35(2):236–43. PMID: 4723033.

91. Roston WL, Whipp BJ, Davis JA, Cunningham DA, Effros RM, Wasserman K. Oxygen uptake kinetics and lactate concentration during exercise in humans. The American review of respiratory disease. 1987; 135(5):1080–4. PMID: 3579007.

92. Wasserman K, Van Kessel AL, Burton GG. Interaction of physiological mechanisms during exercise. J Appl Physiol. 1967; 22(1):71–85. PMID: 6017656.

93. Darrow MD. Ordering and understanding the exercise stress test. American family physician. 1999; 59(2):401–10. Epub 1999/02/04. PMID: 9930131.

94. Wasserman K, Stringer WW, Casaburi R, Koike A, Cooper CB. Determination of the anaerobic threshold by gas exchange: biochemical considerations, methodology and physiological effects. Zeitschrift fur Kardiologie. 1994; 83 Suppl 3:1–12. PMID: 7941654.

95. Gibbons RJ, Balady GJ, Beasley JW, Bricker JT, Duvernoy WF, Froelicher VF, et al. ACC/AHA Guidelines for Exercise Testing. A report of the American College of Cardiology/American Heart Association Task Force on Practice Guidelines (Committee on Exercise Testing). Journal of the American College of Cardiology. 1997; 30(1):260–311. Epub 1997/07/01. PMID: 9207652.

96. Desai KH, Sato R, Schauble E, Barsh GS, Kobilka BK, Bernstein D. Cardiovascular indexes in the mouse at rest and with exercise: new tools to study models of cardiac disease. The American journal of physiology. 1997; 272(2 Pt 2):H1053–61. PMID: 9124413.

97. Caiozzo VJ, Davis JA, Ellis JF, Azus JL, Vandagriff R, Prietto CA, et al. A comparison of gas exchange indices used to detect the anaerobic threshold. Journal of applied physiology: respiratory, environmental and exercise physiology. 1982; 53(5):1184–9. PMID: 7174412.

98. Brooks GA. Mammalian fuel utilization during sustained exercise. Comparative biochemistry and physiology Part B, Biochemistry & molecular biology. 1998; 120(1):89–107. PMID: 9787780.

99. Roberts TJ, Weber JM, Hoppeler H, Weibel ER, Taylor CR. Design of the oxygen and substrate pathways. II. Defining the upper limits of carbohydrate and fat oxidation. The Journal of experimental biology. 1996; 199(Pt 8):1651–8. PMID: 8708572.

100. Wieland OH. The mammalian pyruvate dehydrogenase complex: structure and regulation. Reviews of physiology, biochemistry and pharmacology. 1983; 96:123–70. PMID: 6338572.

101. Putman CT, Jones NL, Lands LC, Bragg TM, Hollidge-Horvat MG, Heigenhauser GJ. Skeletal muscle pyruvate dehydrogenase activity during maximal exercise in humans. The American journal of physiology. 1995; 269(3 Pt 1):E458–68. PMID: 7573423.

102. Krahwinkel W, Ketteler T, Godke J, Wolfertz J, Ulbricht LJ, Krakau I, et al. Dobutamine stress echocardiography. European heart journal. 1997; 18 Suppl D:D9–15. PMID: 9183605.

103. Wiesmann F, Ruff J, Engelhardt S, Hein L, Dienesch C, Leupold A, et al. Dobutamine-stress magnetic resonance microimaging in mice: acute changes of cardiac geometry and function in normal and failing murine hearts. Circulation research. 2001; 88(6):563–9. Epub 2001/04/03. PMID: 11282889.

104. Lujan HL, DiCarlo SE. Cardiac output, at rest and during exercise, before and during myocardial ischemia, reperfusion, and infarction in conscious mice. American journal of physiology Regulatory, integrative and comparative physiology. 2013; 304(4):R286–95. doi: 10.1152/ajpregu.00517.2012 PMID: 23302959; PubMed Central PMCID: PMC3567356.